[DOI]10.12016/j.issn.2096-1456.202550104

·基础研究·

HIF-1α对BMSCs膜片成骨-成血管耦联的效应研究

张丹，　黄银莉，　滕雍辉，　韩畅
银川市口腔医院正畸科，宁夏回族自治区 银川（750000）

【摘要】　目的　探讨低氧诱导因子-1α（hypoxia-inducible factor-1α，HIF-1α）对骨髓间充质干细胞（bone marrow mesenchymal stem cells，BMSCs）膜片成骨-成血管耦联的效应，为体外构建预血管化的组织工程骨提供依据。**方法**　获得医院实验动物伦理委员会批准，体外培养Wistar大鼠的BMSCs，将携带HIF-1α的慢病毒（lentivirus，LV）和空载慢病毒稳定转染至第三代大鼠BMSCs中，形成Lv-HIF-1α-BMSCs组和Lv-BMSCs组，同时以未转染慢病毒的BMSCs为空白对照（BMSCs组），荧光定量PCR和Western Blot验证转染HIF-1α的效果。将LV-HIF-1α-BMSCs进行诱导分化形成内皮样细胞（endothelial-like cells，iECs），光学显微镜观察形态，细胞流式CD31检测分化情况，Transwell实验检测HIF-1α对iECs的迁移能力。将LV-HIF-1α-BMSCs（实验组）和LV-BMSCs（对照组）连续成骨诱导培养形成成骨细胞膜片（osteogenic cell sheets，OCTs），分别在第14、21天进行碱性磷酸酶和茜素红染色、拍照并计数其矿化能力。最终将iECs植入OCTs中构建预血管化的成骨膜片（prevascularized osteogenic cell sheets，P-OCTs），在第1、3、7、14天进行免疫荧光CD31检测并计算内皮血管网形成的数量；第1、7、14天进行骨桥蛋白（osteopontin，OPN）和骨钙素（osteocalcin，OCN）的Western Blot检测，验证其成骨分化的能力。**结果**　慢病毒转染BMSCs的最佳感染复数（multiplicity of infection，MOI）为30，转染率>80%。荧光定量PCR和Western Blot结果显示，与LV-BMSCs组和BMSCs组相比，LV-HIF-1α-BMSCs组中的HIF-1α具有稳定且高的表达（$P<0.05$）。LV-HIF-1α-BMSCs向iECs分化效率高达91.81%。Transwell实验结果显示HIF-1α具有体外招募iECs的作用；碱性磷酸酶染色和茜素红染色证实LV-HIF-1α-BMSCs形成的OCTs具有明显的成骨分化能力，与对照组LV-BMSCs相比差异具有统计学意义（$P<0.05$）。当iECs植入LV-HIF-1α-BMSCs组OCTs中形成P-OCTs时，iECs大量增殖、迁移并快速融合，免疫荧光CD31染色显示进行性管腔和血管网的形成。OPN、OCN的表达与对照组Lv-BMSCs相比显著增强，OPN在第1天表达量最高，OCN在第7天表达量最高（$P<0.05$）。**结论**　HIF-1α增强表达的BMSCs经诱导分化后具有良好的成骨-成血管效应，为优化构建三维预血管化的骨组织提供实验基础。

【关键词】　低氧诱导因子-1α；　骨髓间充质干细胞；　细胞膜片；　预血管化；
成骨-成血管耦联效应；　骨组织工程；　碱性磷酸酶；　茜素红；　骨桥蛋白；　骨钙素
【中图分类号】　R78　**【文献标志码】**　A　**【文章编号】**　2096-1456（2025）09-0744-13
【引用著录格式】　张丹，黄银莉，滕雍辉，等. HIF-1α对BMSCs膜片成骨-成血管耦联的效应研究[J]. 口腔疾病防治，2025，33(9)：744-756. doi:10.12016/j.issn.2096-1456.202550104.

微信公众号

Effect of HIF-1α on osteogenic-angiogenic coupling response in BMSCs sheets

ZHANG Dan, HUANG Yinli, TENG Yonghui, HAN Chang.　Department of Orthodontics, Yinchuan Stomatology Hospital, Yinchuan 750000, China
Corresponding author: ZHANG Dan, Email:1254887917@qq.com

【Abstract】　Objective　To explore the effect of HIF-1α on osteogenic - angiogenic coupling response in bone mesenchymal stem cells (BMSCs) and provide new concepts for engineered bone tissue *in vitro*. **Methods**　With the approval of the hospital's experimental animal ethics committee, BMSCs were harvested from Wistar rats. The lentivirus

【收稿日期】2025-03-15；　**【修回日期】**2025-06-10
【基金项目】宁夏回族自治区自然科学基金（2023AAC03880）
【通信作者】张丹，主治医师，硕士，Email:1254887917@qq.com

carrying hypoxia-inducible factor-1α (HIF-1α) and empty lentivirus were stably transfected into the third generations of BMSCs to form LV-HIF-1α-BMSCs and LV-BMSCs. Meanwhile, BMSCs without transfection of lentivirus were used as a blank control. Then, the effect of HIF-1α transfection was verified by qPCR and Western Blot. LV-HIF-1α-BMSCs were induced to differentiate into endothelium-like cells (iECs). The morphology was observed by optical microscopy, the differentiation rate was detected by cellular flow CD31, and the Transwell test was used to detect the migration ability. At the same time, LV-HIF-1α-BMSCs and LV-BMSCs were continuously cultured to form osteogenic cell sheets (OCTs), which were stained by alkaline phosphatase on day 14 and alizarin red staining on day 21, and counted for mineralization capacity. Finally, iECs were implanted into OCTs to form prevascularized osteogenic cell sheets (P-OCTs), immunofluorescence CD31 was performed to detect the formation of vascular networks, and the results were recorded on days 1, 3, 7, and 14. Meanwhile, osteopontin (OPN) and osteocalcin (OCN) were detected by western blot to verify their ability for osteogenic differentiation on days 1, 7, and 14. **Results**　The optimal multiplicity of infection (MOI) for lentiviral transfection was 30, and the transfection efficiency was >80%. The results of qPCR and western blot showed that compared with the LV-BMSCs group and BMSCs group, the LV-HIF-1α-BMSCs group had stable and high expressions of HIF-1α (P<0.05). LV-HIF-1α-BMSCs showed an enhanced ability to differentiate into endothelial cells, with a differentiation rate as high as 91.81%. Transwell assay verified that HIF-1α could recruit iECs *in vitro*. Alkaline phosphatase staining and alizarin red staining confirmed that OCTs formed by LV-HIF-1α-BMSCs had a statistically significant osteogenic differentiation ability compared with LV -BMSCs control group (P<0.05). When iECs were implanted into the LV-HIF-1α-BMSCs group OCTs to form P-OCTs, iECs substantially proliferated and rapidly fused, and formation of the progressive lumen was revealed by immunofluorescent CD31 staining. The expressions of OPN and OCN were significantly enhanced compared with those of the LV-BMSCs control group; OCN was the highest on day 7, and OPN was the highest on day 1 (P<0.05). **Conclusion**　BMSCs transfected by HIF-1α have good osteogenic-angiogenic effect after induction and differentiation, which provides experimental foundation for optimizing the construction of three-dimensional prevascularized bone tissue.

【Key words】 hypoxia-inducible factor-1α; bone marrow mesenchymal stem cells; cell sheet; prevascularization; osteogenic-angiogenic coupling response; bone tissue engineering; alkaline phosphatase staining; alizarin red staining; osteopontin; osteocalcin

J Prev Treat Stomatol Dis, 2025, 33(9): 744-756.

【Competing interests】 The authors declare no competing interests.

This study was supported by the grants from Natural Science Foundation of Ningxia Hui Autonomous Region (No. 2023AAC03880).

利用骨髓间充质干细胞(bone mesenchymal stem cells, BMSCs)为种子细胞形成的干细胞膜片成功在体外构建了组织工程骨,为骨的缺损修复提供治疗策略[1-4]。同时,该策略也面临着血管化问题。研究显示,宿主血管弥散作用供给氧气和营养物质的距离为100~200 μm;而组织工程移植物尺寸为0.1~10 cm,因此植入体内后缺乏有效的氧供应[5-6]。研究表明,体外构建的组织工程骨植入体内后,由于自身血管生成匮乏、血管整合不足导致移植物血供不充分、新生骨形成缓慢,最终导致移植失败的发生[7-8]。即使体外构建了预血管化,其存活也取决于与宿主血管的连接和灌注,而这个过程往往需要数天到数周的时间[6,9]。因此,如何促进和稳定组织工程骨内新生血管的形成,并快速而有效地与宿主血管整合是目前亟待解决的难题。

在骨缺损区,成血管-成骨耦联反应是多因素参与的复杂而精准的调控过程,大量研究表明[10-12],低氧诱导因子-1α(hypoxia-inducible factor-1α, HIF-1α)在此过程中发挥了核心的调控作用。HIF-1α不仅能激活、招募和调控宿主细胞向损伤部位迁移、增殖、分化,还能诱导血管网出芽、塑形、吻合,并促进新骨生成[13-15]。然而,HIF-1α受机体严格的调控,存在半衰期短、易降解、稳定性差等劣势[16]。研究发现,通过低氧环境,缺氧模拟剂,或基因工程等方式可提高HIF-1α的表达,发挥相应的靶向调控作用,从而促进骨和血管的生成[17-20]。

因此,本研究拟利用基因增强技术将HIF-1α稳定转染至大鼠BMSCs中,体外构建预血管化的

成骨膜片。通过稳定和持续表达的HIF-1α，研究膜片内成血管-成骨耦联反应，以期为骨缺损修复提供全新的治疗策略，促进骨组织再生医学的发展。

1　材料和方法

1.1　实验动物

出生2~3周Wistar大鼠6只，雌雄不限，体重40~60 g，购于江西中洪博元生物技术有限公司，合格证号SYXK（赣2020-0001）。本实验经医院实验动物伦理委员会批准（审批号：YCKQLL2022018）。

1.2　主要材料与仪器

慢病毒HIF-1α过表达载体（NM_024359.2，cds：327.2807，安徽通用生物系统有限公司，中国），Trizon Reagent（CW0580S，CWBIO，中国），超纯RNA提取试剂盒（CW0581M，CWBIO，中国），反转录及定量试剂盒（Takara，日本），HiScript II Q RT SuperMix for qPCR（+gDNA wiper）（R223-01，Vazyme，中国），SuperStar Universal SYBR Master Mix（CW3360M，CWBIO，中国），兔抗鼠CD31单克隆抗体（25-0310-82，赛默飞，中国），一抗兔抗鼠CD31（GB11063-2，Servicebio，中国），二抗Cy3山羊抗兔IgG（H+L）（AS007，ABclonal，中国），即用型DAPI染液（KGA215-50，凯基生物，中国），兔抗鼠OCN抗体（A20800，ABclonal，中国），兔抗鼠OPN抗体（YT3467，Immunoway，中国），HRP标记山羊抗兔IgG（H+L）（GB23303，Servicebio，中国），胎牛血清FBS（四季青，上海，中国），L-DMEM、H-DMEM、M199培养基（Hyclone，美国），PBS（KGB5001，凯基生物，中国），青链霉素混合液（100×）细胞培养专用（双抗）（P1400，Solarbio，中国），L-谷氨酰胺（200 mmol/L）（G0200，Solarbio，中国），血管内皮生长因子（vascular endothelial growth factor，VEGF）（HY-P7311，MCE，中国），成纤维生长因子（fibroblast growth factor，FGF）（HY-P7091，MCE，中国），碱性磷酸酶染色液（G1481，Solarbio，中国），茜素红S染液（G1038，Servicebio，中国），倒置相差显微镜（Olympus，日本），荧光显微镜（Olympus，日本），恒温培养箱（精宏GNP9050，上海，中国），普通PCR扩增仪（TC-EA，杭州博日，中国），荧光PCR仪（CFX Connect™实时，Bio-Rad，中国），NovoCyte™流式细胞仪（NovoCyte 2060R，杭州艾森，中国），高速台式冷冻离心机（H1750R，湖南湘仪，中国）。

1.3　实验方法

1.3.1　原代BMSCs的分离和培养　采用全骨髓贴壁法分离培养Wistar大鼠BMSCs。将出生2~3周Wistar大鼠拉颈处死，75%酒精浸泡消毒15 min；无菌条件下完整剥离双侧股骨和胫骨，无菌PBS漂洗2~3次；眼科剪剪断干骺端，显露骨髓腔，用5 mL注射器吸取3~4 mL L-DMEM培养液反复冲洗骨髓腔，将收集的骨髓悬液置于15 mL离心管中，转速1 000 r/min下离心5 min；去除上清液，用5 mL含10% FBS的L-DMEM完全培养液重悬，将细胞悬液转移至25 cm^2培养瓶，放置于37 ℃、5%的CO^2饱和湿度培养箱中静置培养；72 h后全量换液；以后每2~3 d换液，去除未贴壁细胞。上述细胞培养期间，倒置相差显微镜观察细胞的生长和形态。

1.3.2　携带HIF-1α的慢病毒（lentivirus，LV）转染BMSCs　将培养的第三代BMSCs进行胰酶消化，制成浓度为1×10^5/mL的细胞悬液，将细胞悬液按1 mL/孔接种于12孔板中，放置于37 ℃、5%的CO^2饱和湿度培养箱中静置培养，待细胞融合度>80%，按预实验感染复数MOI值=30加入适当的病毒量。实验组为携带HIF-1α基因的慢病毒转染BMSCs，即LV-HIF-1α-BMSCs组；阴性对照组为空载慢病毒转染BMSCs，即LV-BMSCs组；空白对照组为未转染慢病毒的BMSCs，即BMSCs组。转染后，利用荧光定量PCR和Western Blot验证HIF-1α的转染率。

荧光定量PCR操作步骤：使用Trizol提取RNA，根据HiScript II Q RT SuperMix for qPCR逆转录试剂盒操作制备cDNA，然后进行qPCR检测。HIF-1α基因检测反应条件：变形，95 ℃ 10 s，退火，58 ℃ 30 s，延伸，72 ℃ 30 s，40个循环。实验重复3次，最后计算HIF-1α的平均表达量。引物序列见表1。

表1　PCR引物序列

Table 1　Primer sequence of PCR

Primers	Sequence（5'-3'）	Length/bp	Temperature/℃
GAPDH	F: GACAACTTTGGCATCGTGGA	133	58.0
	R: ATGCAGGGATGATGTTCTGG		
HIF-1α	F: CTAAAGGACAAGTCACCACAGG	314	58.7
	R: TAGCAGAGTCAGGGCATCG		

HIF-1α: hypoxia induced factor 1α

Western Blot实验步骤：弃掉培养皿中培养液，加入200 μL RIPA细胞裂解液，12 000 r/min高速离心机离心10 min，取上清液，BCA蛋白定量试剂盒测定HIF-1α浓度，10% SDS-PAGE电泳分离后转至PVDF膜，用1×TBST配置3%的脱脂牛奶封闭

液，封闭1 h，加入一抗兔抗HIF-1α（bs-0737R，Bioss，1/1 000））孵育过夜，洗膜，用1×TBST浸泡15 min后弃掉1×TBST，重复3次，再加入二抗HRP偶联山羊抗兔IgG（H+L）（GB23303，Servicebio，1/2 000））孵育2 h，清洗后，加入发光液显影成像。

1.3.3 诱导形成内皮样细胞（endothelial-like cells，iECs） 将LV-HIF-1α-BMSCs置于内皮诱导液（包含：M199培养基，10%FBS，100 U/mL青链霉素，0.29 g/L谷氨酰胺，10 μg/L rVEGF，2 μg/L rbFGF）连续14 d诱导分化下形成iECs，流式细胞仪检测内皮细胞特殊表面标志物CD31的表达量。LV-HIF-1α-BMSCs置于非内皮诱导液（包含：M199培养基，10%FBS，100 U/mL青链霉素）的培养为对照组。

1.3.4 iECs的细胞迁移实验 将LV-HIF-1α-BMSCs以$1\times10^5/cm^2$的密度接种至24孔板连续培养形成膜片，Transwell上室内接种iECs（1×10^5/mL，100 μL），下室内加入600 μL H-DMEM完全培养基（包括：H-DMEM培养基，10%FBS），移入孵箱内静置培养24 h。取出后，擦除上室内未迁移的iECs，4%多聚甲醛固定小室30 min，1%医用甲紫溶液用PBS稀释（1∶40）后对下室壁内的迁移细胞进行染色15 min，PBS冲洗3遍，显微镜下观察并计数迁移细胞的数量。24孔板内接种相同密度的LV-BMSCs为对照组。

1.3.5 成骨分化细胞膜片的构建 将LV-HIF-1α-BMSCs以$1\times10^5/cm^2$的密度接种至6孔板中，连续培养形成的干细胞膜片在成骨诱导液（包含：H-DMEM培养基，10%FBS，10 mmol/L甘油磷酸钠，10 nmol/L地塞米松，50 mg/L抗坏血酸）的培养下进行成骨分化，形成成骨细胞膜片（实验组）。LV-BMSCs形成的成骨膜片为对照组。在成骨诱导的第14 d进行碱性磷酸酶染色检测早期成骨分化的情况；第21 d进行茜素红染色检测钙结节形成。

1.3.6 预血管化的成骨膜片的构建 将iECs以$5\times10^4/cm^2$的密度种植到成骨膜片上继续培养，构建预血管化的成骨膜片。分别在iECs植入后的第1、3、7、14天，进行CD31免疫荧光染色，荧光显微镜观察血管网络形成特征，并定量计数血管网形成的数量。第1、7、14天对成骨特异性蛋白骨桥蛋白（osteopontin，OPN）和骨钙素（osteocalcin，OCN）进行Western Blot定量检测。将iECs接种至LV-HIF-1α-BMSCs成骨膜片为实验组，接种至LV-BMSCs成骨膜片为对照组。

CD31免疫荧光操作步骤：PBS冲洗细胞膜片3次，4%多聚甲醛固定15 min，PBS冲洗3次，加入5% BSA，室温下封闭30 min。移液枪吸干封闭液，加入足量一抗兔抗CD31，4 ℃冰箱过夜。室温复温45 min，PBS浸洗3次，加入荧光二抗Cy3山羊抗兔IgG（H+L），室温避光孵育30 min。PBS充分淋洗后，滴加DAPI对样本进行核染，避光孵育3 min。PBS冲洗，50%甘油封闭样本，免疫荧光显微镜下观察并采集图像（DAPI紫外激发波长330~380 nm，发射波长420 nm，发蓝光；CY3激发波长510~560 nm，发射波长590 nm，发红光）。

Western Blot操作步骤：同上，目的一抗兔抗鼠OCN，目的一抗兔抗鼠OPN，二抗HRP标记山羊抗兔IgG（H+L）。

1.4 统计学方法

采用SPSS22.0软件分析实验数据，使用GraphPad Prism8.0.2软件绘制统计图。两组间比较采用独立样本t检验，多组间比较采用方差分析，$P<0.05$为差异有统计学意义。

2 结 果

2.1 慢病毒转染效率检测

将生长良好的第三代BMSCs进行慢病毒转染，经过前期预实验发现，慢病毒转染BMSCs的最佳感染复数MOI值=30时，荧光显微镜下观察绿色荧光蛋白阳性率>80%（图1a）。荧光定量PCR（图1 b）和Western Blot（图1c、1d）结果显示，与LV-BMSCs组和BMSCs组相比，LV-HIF-1α-BMSCs组中的HIF-1α具有稳定且高的表达（$P<0.05$）。

2.2 iECs的培养及鉴定

LV-HIF-1α-BMSCs在内皮诱导液下连续14 d诱导培养，形成iECs。显微镜下观察LV-HIF-1α-BMSCs生长密集，呈长梭形或纺锤状（图2a），而iECs呈卵圆形或扁圆形，似“铺路石”样外观（图2b）。使用流式细胞仪检测内皮细胞表面分化标志物CD31（图2c、2d），结果显示：分化组中的LV-HIF-1α-BMSCs在内皮诱导液的诱导分化下转化率高达91.81%，而在置于非内皮诱导液的LV-HIF-1α-BMSCs对照组的转化率仅为0.81%，差异具有统计学意义（图2e，$P<0.05$）。Transwell实验结果表明，在对照组LV-BMSCs中基本无iECs迁移（图2f），实验组LV-HIF-1α-BMSCs组中的iECs发生了大量的迁移（图2g），迁移量为每个视野下平均400个iECs，证实了HIF-1α具有体外招募iECs的作用（$P<0.05$）（图2h）。

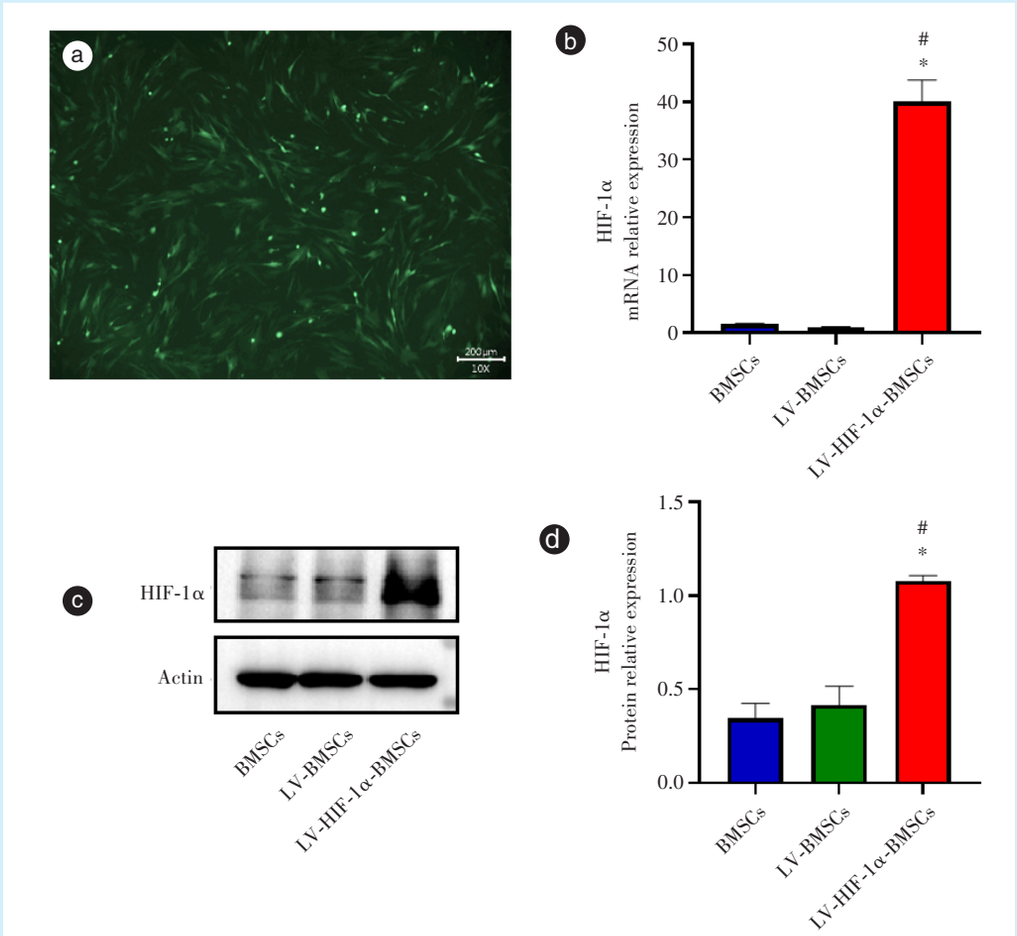

a: fluorescence microscopy showed that the expression of green fluorescent protein was >80%; b: qPCR of HIF-1α to LV-HIF-1α-BMSCs, LV-BMSCs, and BMSCs, and the HIF-1α mRNA was highest in the LV-HIF-1α-BMSCs group; c: Western Blot of HIF-1α to LV-HIF-1α-BMSCs, LV-BMSCs, and BMSCs; d: the HIF-1α protein was highest in the LV-HIF-1α-BMSCs group. *: compared with the BMSCs group, $P<0.05$; #: compared with the LV-BMSCs group, $P<0.05$. The BMSCs blank control group: bone marrow mesenchymal stem cells that were not transfected with lentivirus; the LV-BMSCs negative control group: empty lentivirus-transfected bone marrow mesenchymal stem cells; the LV-HIF-1α-BMSCs experimental group: lentivirus carrying hypoxia-inducible factor-1α transfected bone marrow mesenchymal stem cells. BMSCs: bone marrow mesenchymal stem cells; HIF-1α: hypoxia-inducible factor-1α

Figure 1　The detection of HIF-1α in lentivirus-transfected BMSCs by qPCR and Western Blot

图 1　qPCR 和 Western Blot 检测慢病毒转染 BMSCs 后 HIF-1α 的表达

2.3　成骨膜片的构建和成骨能力的检测

在成骨诱导液的连续培养下，LV-HIF-1α-BMSCs 大量增殖分化形成致密的成骨膜片，肉眼可见膜片上呈颗粒状，系钙盐沉积所致（图 3a）。显微镜下观察成骨膜片（图 3b~3d），随时间推移，大量细胞密集排列，并交织成致密的膜样结构，膜片上可见钙结节沉积。在成骨膜片培养的第 14 天，进行成骨细胞分化的标记物碱性磷酸酶染色，结果显示实验组中出现了大量且明显的钙盐沉积和染色沉淀，差异有统计学意义（$P<0.05$）。在成骨膜片培养的第 21 天，进行茜素红染色显示，实验组中红染的矿化结节更多且更明显，差异有统计学意义（$P<0.05$），见图 3e~3j。

2.4　预血管化成骨膜片中成骨-成血管耦联效应

2.4.1　血管生成效应　免疫荧光 CD31 染色显示（图 4），当 iECs 接种至 LV-HIF-1α-BMSCs 形成的成骨细胞膜片（实验组）的第 1 天时，iECs 大量增殖并在膜片上发生迁移和少量融合，并快速形成空泡样结构（图 4a）。第 3 天时，iECs 在成骨膜片上大量融合，形成管腔样结构（图 4b）；培养至第 7 天时，iECs 的融合达到高峰，形成管腔样结构的数量达到最多（图 4c）；随时间推移，iECs 的融合更加致

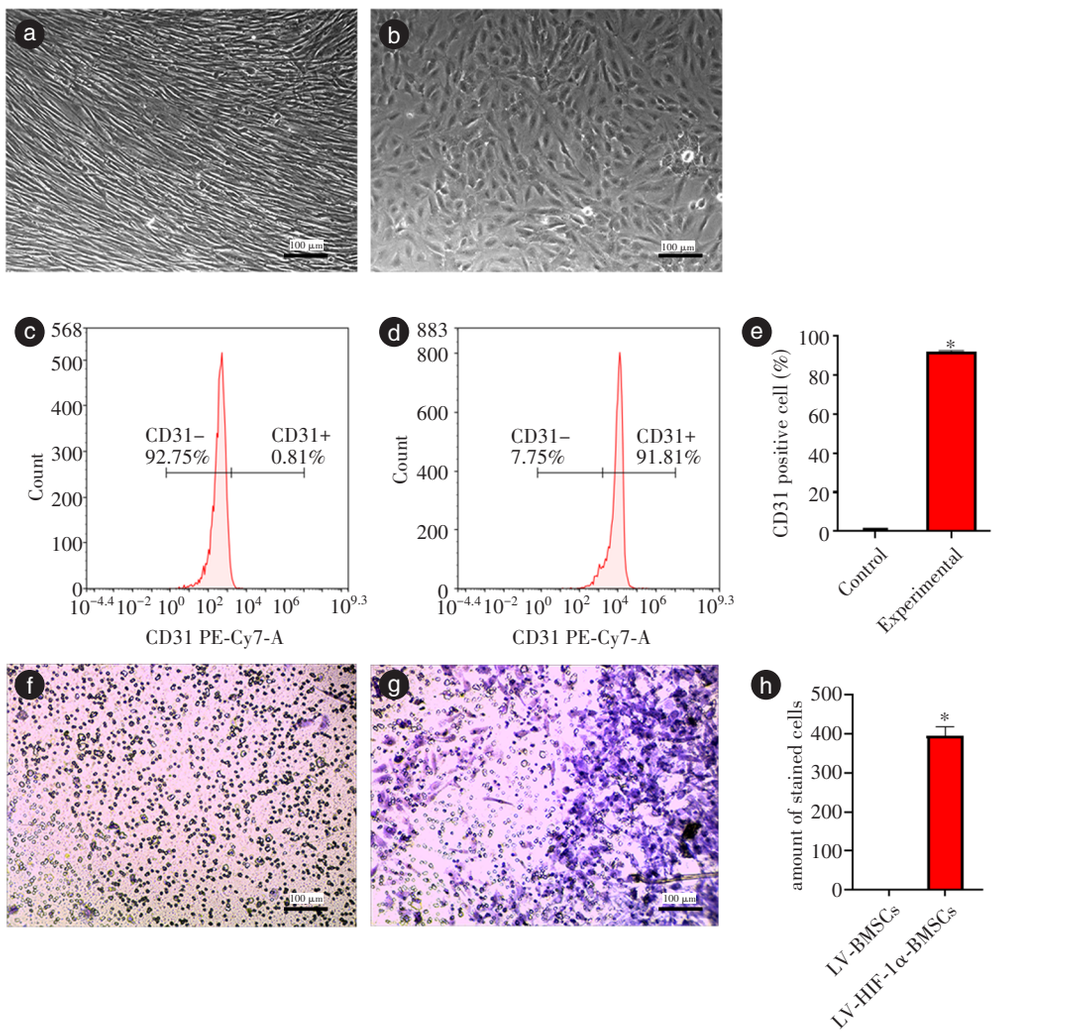

a: LV-HIF-1α-BMSCs were long spindles; b: iECs were oval and cobblestone-like; c: flow cytometry of the control group, with a CD31 positive expression of 0.81%; d: flow cytometry of the experimental group, with a CD31 positive expression of 91.81%; e: flow cytometry results of the statistical analysis. The control group: LV-HIF-1α-BMSCs were cultured in non-endothelial induction medium; The experimental group: LV-HIF-1α-BMSCs were cultured in endothelial induction medium. f & g: the Transwell assay results showed that the LV-BMSCs control group had no migrated iECs (f), and the LV-HIF-1α-BMSCs experimental group had 400 iECs per field of view (g); h: the Transwell assay statistical analysis. *: compared with the control group, $P<0.05$ (scale bars: a, b, f, g = 100 μm). LV-BMSCs: empty lentivirus-transfected bone marrow mesenchymal stem cells; LV-HIF-1α-BMSCs: lentivirus carrying hypoxia-inducible factor-1α transfected bone marrow mesenchymal stem cells; iECs: endothelial-like cells that were induced from lentivirus carrying hypoxia-inducible factor-1α transfected bone marrow mesenchymal stem cells; BMSCs: bone marrow mesenchymal stem cells; HIF-1α: hypoxia-inducible factor 1α

Figure 2　The cell culture, identification and migration ability of iECs

图2　iECs的培养、鉴定及迁移能力的检测

密，形成的管腔样结构也更稳定（图4d）。然而，iECs在LV-BMSCs形成的成骨细胞膜片（对照组）上的迁移和融合均较实验组缓慢，形成的血管空泡和管腔样结构也较少。在培养的第7 d，形成的管腔样结构数量达到峰值。但管腔样结构并不稳定，随时间推移而明显下降。统计学分析显示，在任一时间上，实验组中内皮血管网的数量均明显高于对照组（$P<0.05$），且各组中内皮血管网的数量于第7 d达峰值（$P<0.05$，图4e~4i）。

2.4.2　骨生成效应　对成骨特异性基质蛋白OCN、OPN的Western Blot检测显示，OCN在LV-HIF-1α-BMSCs实验组中的表达随时间推移而增加，并在培养的第7天达到峰值，后又随时间的推移而降低，而在LV-BMSCs对照组中OCN的表达在

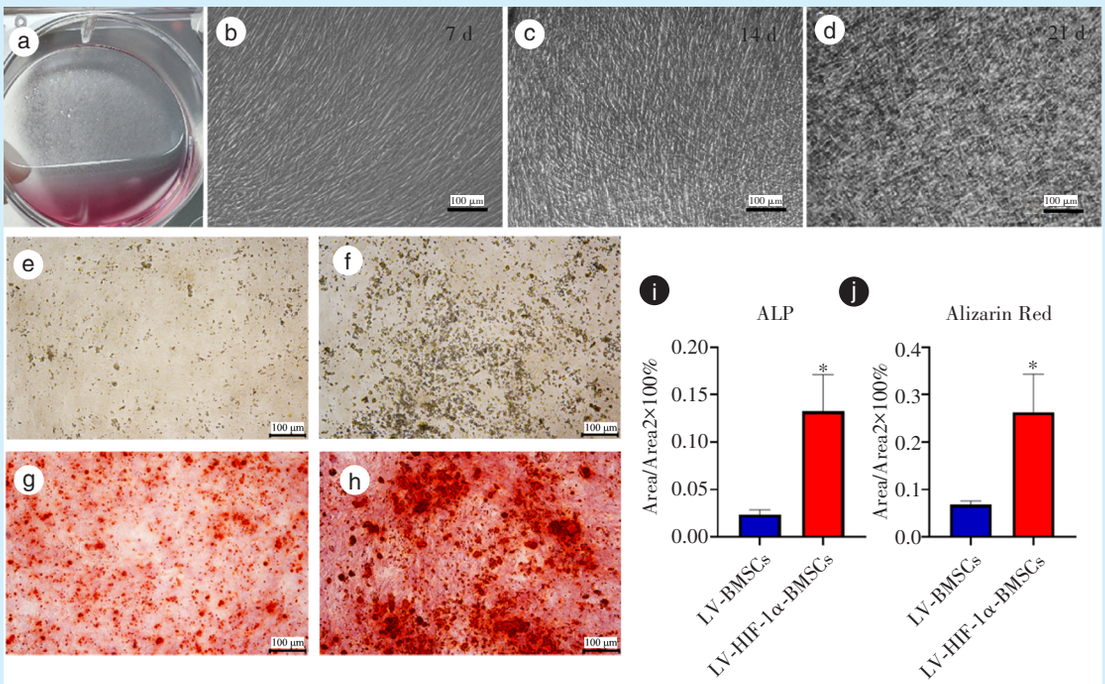

a: the view of osteogenic cell sheets, which formed a dense and turbid film. b-d: the microscopic morphology of osteogenic cell sheets on days 7, 14, and 21, showing the formation of calcium nodules over time. e: ALP staining results of the LV-BMSCs control group on day 14; f: ALP staining results of the LV-HIF-1α-BMSCs experimental group on day 14. A large and obvious deposition of calcium salts and staining precipitates in the experimental group. g: Alizarin red staining results of the LV-BMSCs control group on day 21; h: Alizarin red staining results of the LV-HIF-1α-BMSCs experimental group on day 21. More evident mineralized nodules were stained red in the experimental group. i & j: The statistical analysis of ALP and Alizarin red staining, *: compared with the LV-BMSCs control group, $P<0.05$ (scale bars: b-h=100 μm). The LV-BMSCs control group: empty lentivirus-transfected bone marrow mesenchymal stem cells formed osteogenic cell sheets; the LV-HIF-1α-BMSCs experimental group: lentivirus carrying hypoxia-inducible factor-1α transfected bone marrow mesenchymal stem cells formed osteogenic cell sheets. ALP: alkaline phosphatase staining; BMSCs: bone marrow mesenchymal stem cells; HIF-1α: hypoxia-inducible factor 1α

Figure 3　The effect of HIF-1α on osteogenic ability in osteogenic cell sheets shown by ALP and Alizarin red staining

图3　碱性磷酸酶和茜素红染色检测HIF-1α对成骨膜片成骨能力的影响

实验的第1天时为峰值，并随时间而逐渐降低；另一方面，OPN的表达在实验组的第1天时最高，并随时间的推移而降低，而在LV-BMSCs对照组中的表达也如此。统计学分析显示，在LV-HIF-1α-BMSCs实验组中OCN、OPN的表达均高于LV-BMSCs对照组，且两组在不同时间点的表达差异均具有统计学意义（图5，$P<0.05$）。

3　讨　论

在骨缺损部位，局部低氧环境下，HIF-1α通过调控相关目的基因和宿主体内的前体细胞、干细胞等对成骨-成血管耦联反应发挥了至关重要的作用和意义[15]。本研究通过将HIF-1α稳定转染至大鼠BMSCs中，经过至少14 d的连续成骨诱导获得了成骨细胞膜片；又将LV-HIF-1α-BMSCs连续诱导14 d形成内皮样细胞，利用Transwell细胞迁移实验证实了HIF-1α具有体外招募iECs的作用。将内皮样细胞与成骨细胞膜片共培养，体外成功构建了预血管化的成骨膜片。实验结果证实了HIF-1α促进成骨的效应，以及内皮样细胞在成骨膜片上增殖、迁移并快速融合，进而形成大量的血管空腔和丰富且稳定的三维预血管化网络。

骨的缺损修复仍然是目前临床治疗的难题。自体骨移植作为骨修复的金标准，存在供体有限、供区并发症多、术后感染等问题[21-23]。然而，目前的手术策略未能满足促进血管化骨再生的临床需求，因此会导致移植失败的发生[24]。组织工程技术的发展为骨缺损提供了新思路，大量研究证实了组织工程骨的再生修复能力，然而血管化问题仍然是制约其发展的瓶颈[25-27]。在众多血管化策略的研究中，预血管化的干细胞膜片技术显示巨大的潜力。研究发现[28-30]，以BMSCs为种子细胞

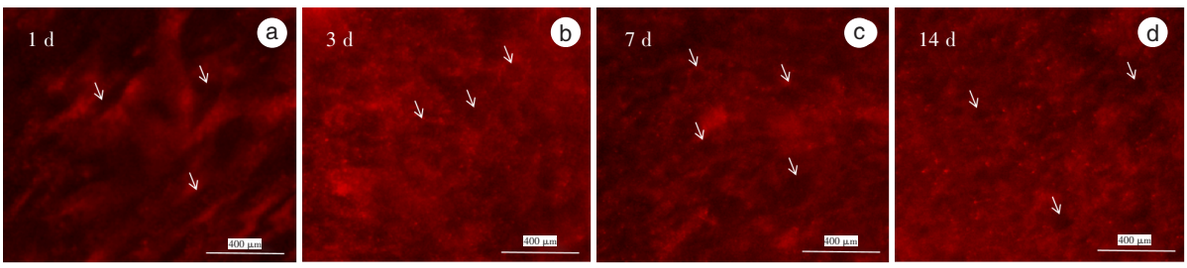
1 d
a
3 d
b
7 d
c
14 d
d
400 μm

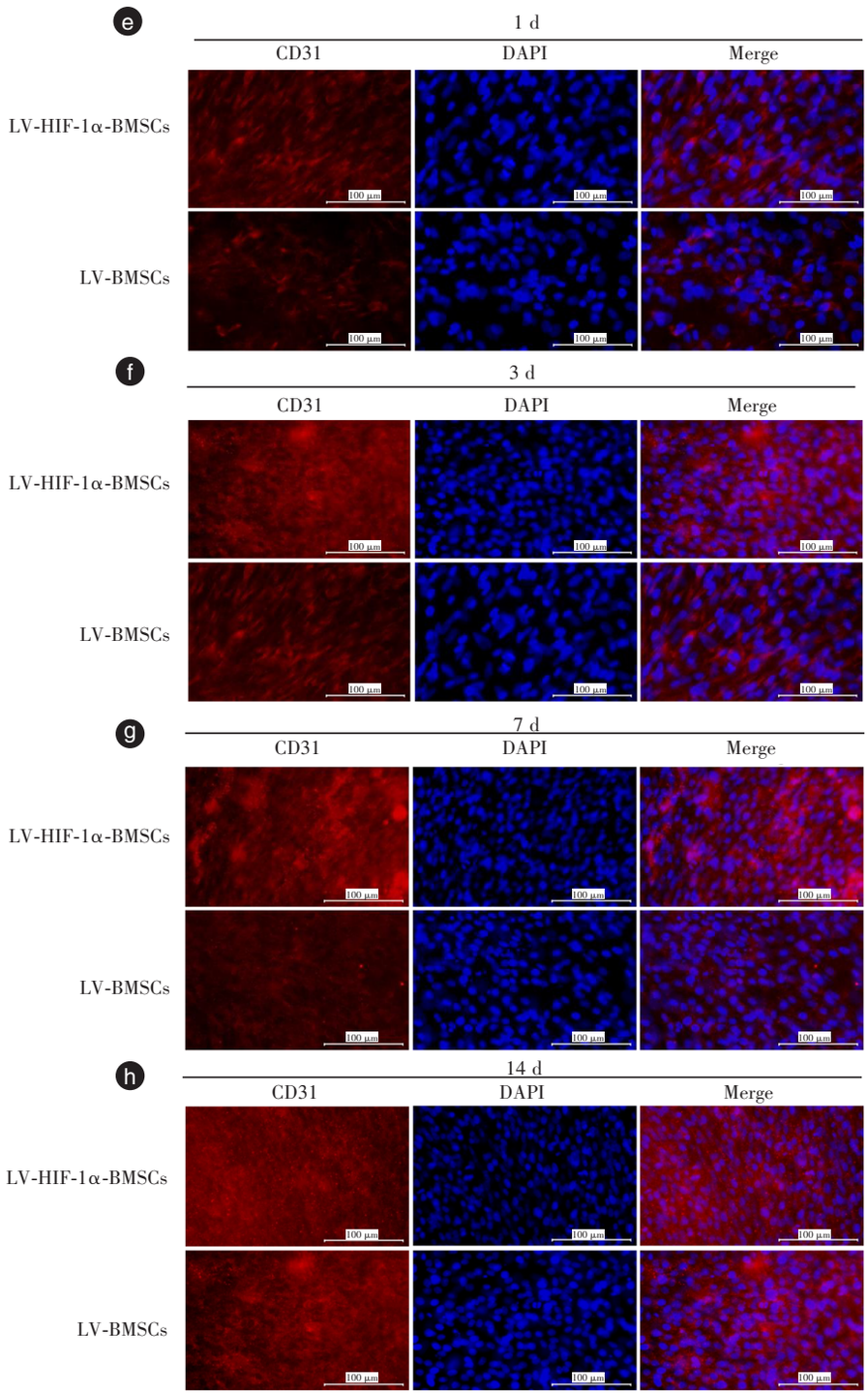
e
1 d
CD31
DAPI
Merge
LV-HIF-1α-BMSCs
LV-BMSCs
f
3 d
g
7 d
h
14 d
100 μm

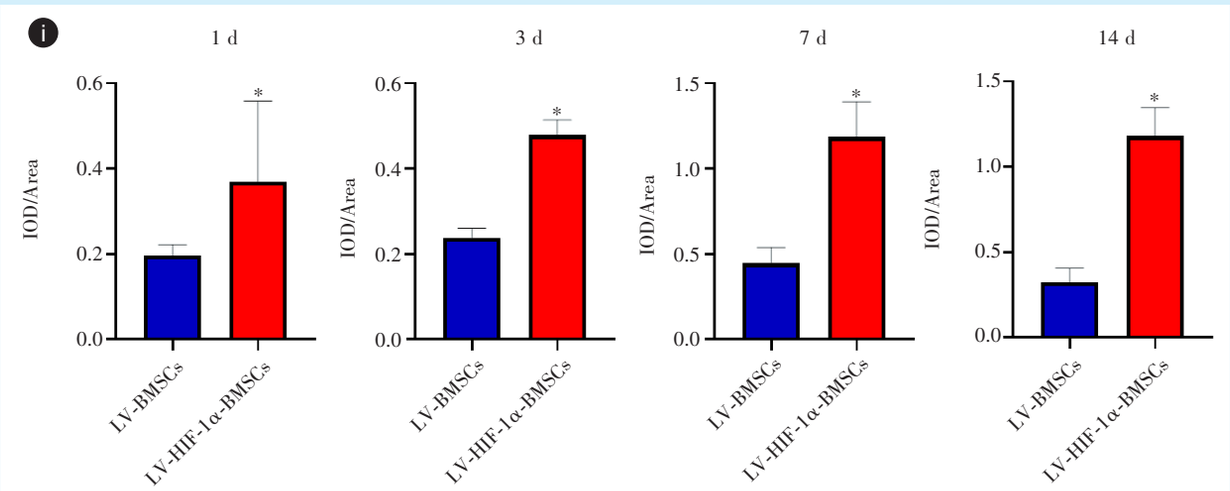

a-d: magnified images of the experimental group on days 1, 3, 7, and 14. The closed loop or branch network formed by continuous CD31+ signal was defined as a vacuole structure (a, white arrow), while the hollow structure was defined as a tubular structure (b - d, white arrow). e-h: CD31 immunofluorescence staining, DAPI, and merged images of the LV-HIF-1α-BMSCs experimental group and LV-BMSCs control group on days 1, 3, 7, and 14. iECs adhered and extensively proliferated on osteogenic cell sheets in the LV-HIF-1α-BMSCs experimental group, and they then migrated and aligned with each other. The vacuole structure was formed on day 1, and the tubular structure was formed on day 3. This structure reached a peak on day 7 and remained stable on day 14. At the same time, the growth of vacuole and tubular structures was restricted in the LV-BMSCs control group. The formation of networks increased over time, reaching a peak on day 7 (scale bars: 100 μm). i: the result of statistical analysis at different time points between the two groups, *: compared with the LV-BMSCs control group, $P<0.05$. The LV-BMSCs control group: the prevascularized osteogenic cell sheets formed by iECs and empty lentivirus-transfected bone marrow mesenchymal stem cells. The LV-HIF-1α-BMSCs experimental group: the prevascularized osteogenic cell sheets formed by iECs and lentivirus carrying hypoxia-inducible factor-1α transfected bone marrow mesenchymal stem cells. iECs: endothelial-like cells that were induced from lentivirus carrying hypoxia-inducible factor-1α transfected bone marrow mesenchymal stem cells; BMSCs: bone marrow mesenchymal stem cells; HIF-1α: hypoxia-inducible factor 1α; DAPI: destination access point identifier

Figure 4　The effect of HIF-1α on angiogenesis in prevascularized osteogenic cell sheets shown by CD31 immunofluorescence staining and DAPI

图4　免疫荧光CD31染色和DAPI检测HIF-1α对预血管化成骨膜片血管生成能力的影响

的细胞膜片技术保留了完整且丰富的细胞外基质成分(extracellular matrix, ECM),建立了充分的细胞-细胞,细胞-基质的信号传导,为血管的长入提供了微环境。Chen等[31]研究发现,当人脐静脉内皮细胞(human umbilical vein endothelial cells, HUVECs)按密度接种到BMSCs膜片时,HUVECs发生迁移、重排并显示了血管化的能力,从而实现了体外预血管化膜片的构建。在本研究中利用LV-HIF-1α-BMSCs连续诱导14 d可获得内皮样细胞,且转化率高达91.81%。而课题组前期实验证实未转染慢病毒的BMSCs诱导形成内皮样细胞的转化率仅为35.1%[32]。因此,LV-HIF-1α-BMSCs的应用不仅弥补了体外培养内皮细胞精度差、周期长的缺点,还为开展体外预血管化提供了充足的细胞保障。利用免疫荧光CD31染色可观察到沿血管内皮细胞膜连续或点状分布的阳性信号,代表了内皮细胞的排列、走向和血管的生成情况[33-34]。研究还表明,当间充质干细胞与内皮细胞共培养时,可上调胶原蛋白基因和平滑肌标记物的表达,激活Notch信号通路促进血管生成[35-36]。然而,在缺血缺氧的环境下,体外构建的预血管化的工程化骨组织移植进入体内后仍然会出现一些问题,如新生血管数量不足且结构不稳定、与宿主血管吻合缓慢,最终导致新骨形成不足,修复效果不理想等[7-8]。

成骨-成血管耦联反应是多基因参与的复杂且精准的调控过程,研究发现HIF-1α在其中发挥了重要的作用[15]。一方面,HIF-1α可调控多种编码血管生成的基因表达,如VEGF、PDGF、Ang-1,2等[37]。其中,VEGF在血管生成的调节中发挥了十分重要的作用,研究表明,HIF-1α/VEGF通路可参与炎症、缺血再灌注、血管生成和重塑等病理生理

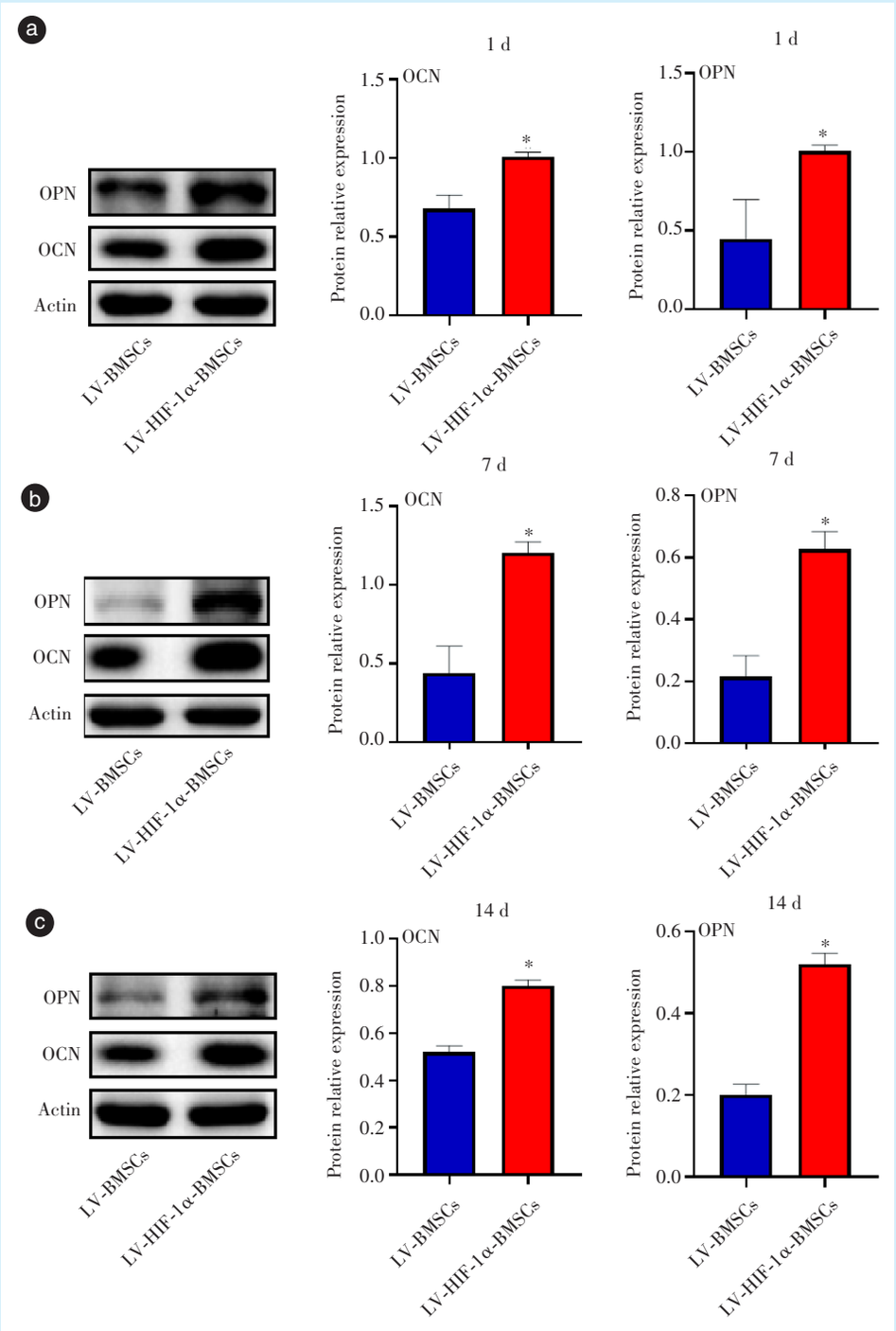

a:Western Blot and statistical analysis of OPN and OCN on day 1; b: Western Blot and statistical analysis of OPN and OCN on day 7; c: Western Blot and statistical analysis of OPN and OCN on day 14. The expressions of OCN and OPN in LV-HIF-1α-BMSCs experimental group were higher than the LV-BMSCs control group; OCN was highest on day 7 and OPN was highest on day 1, *: compared with the LV-BMSCs control group, $P<0.05$. The LV-BMSCs control group: the prevascularized osteogenic cell sheets formed by iECs and empty lentivirus-transfected bone marrow mesenchymal stem cells. The LV-HIF-1α-BMSCs experimental group: the prevascularized osteogenic cell sheets formed by iECs and lentivirus carrying hypoxia-inducible factor-1α transfected bone marrow mesenchymal stem cells. iECs: endothelial-like cells that were induced from lentivirus carrying hypoxia-inducible factor-1α transfected bone marrow mesenchymal stem cells. OPN: osteopontin; OCN: osteocalcin; BMSCs: bone marrow mesenchymal stem cells; HIF-1α: hypoxia-inducible factor 1α

Figure 5　The effect of HIF-1α on the expressions of OCN and OPN in prevascularized osteogenic cell sheets shown by Western Blot

图5　Western Blot检测HIF-1α对预血管化成骨膜片OCN, OPN表达的影响

过程，并在血管生成素-1，2的共同参与调节下，抑制金属蛋白酶组织抑制剂-3的表达，从而介导骨和血管的生成[11, 38]。同时，HIF-1α/VEGF通路可诱导BMSCs向成骨细胞分化，促进内皮细胞的增殖、迁移，进一步促进骨和血管的生成[39-41]。此外，Transwell细胞迁移实验证实了HIF-1α具有体外招募iECs的作用，而此调节机制与HIF-1α下游目的基因CXC趋化因子家族有关。HIF-1α是介导内皮祖细胞（endothelial progenitor cell，EPC）促进血管修复和新生中不可或缺的介质，其作用包括调控EPC的存活、分化、动员，以及多种血管生成因子将EPC迁移、招募和黏附到损伤部位[42]。在对糖尿病伤口愈合的研究中发现，HIF-1α通过激活巨噬细胞和成纤维细胞中的VEGF和趋化因子CXCL12/基质细胞衍生因子（stromal-derived factor-1，SDF-1α）的表达，在新生血管的形成中发挥了重要的作用，其中VEGF用于激活从骨髓到外周循环中的EPC，而CXCL12/SDF-1α可诱导EPC向受损区域的迁移和招募[43]。研究显示[44]，VEGF可增加CXCR4（CXCL12受体）在内皮细胞上的表达，从而增强了CXCL12促进血管生成的特性。在本研究中，实验组的iECs在成骨膜片上大量增殖、迁移并快速融合形成管腔样结构，而对照组的血管形成速度、数量及稳定性均不如实验组。因此，涉及HIF-1α诱导血管生成的分子机制值得未来更进一步的研究。

利用LV-HIF-1α-BMSCs连续成骨诱导形成成骨细胞膜片，成骨细胞膜片的ECM中含有大量的骨胶原和非胶原蛋白，如Ⅰ型胶原、骨桥素、骨钙素，纤连蛋白、蛋白聚糖等[45-46]，可介导整合素、基质金属蛋白酶、转化生长因子-β、Wnt等家族的信号通路，调控成骨细胞的增殖和分化，并促进血管的出芽和生长，从而进一步促进骨的再生修复[46-48]。研究还发现，骨生成细胞可分泌VEGF等因子促进血管的生成，而血管生成细胞也可分泌骨形态发生蛋白-2，4等因子促进骨的生成[49]。由此可见，骨再生与血管形成之间存在密切的联系。然而，在预血管化的成骨膜片上，对成骨特异性基质蛋白OCN、OPN的Western Blot检测发现，实验组中OCN、OPN的表达均高于对照组，OCN的表达在第7天最高，然而OPN的表达却随时间而下降。分析可能的原因是成骨膜片的老化和培养环境的限制。本研究利用6孔板培养成骨膜片，而成骨膜片的形成条件为连续不传代培养至少14 d，因此有限的空间会造成膜片的老化和卷曲，甚至脱落。并且，后续又将内皮样细胞种植到成骨膜片上，继续开展HIF-1α对成骨-成血管耦联反应的效应研究，而培养空间的限制会加速膜片的老化可能会影响实验的结果。因此，本课题组会继续探索共培养的时间点，寻找HIF-1α调控成骨-血管反应的最佳时机；另一方面，考虑利用支架材料或微凝胶组装体系，为成骨细胞和血管的长入提供有力的条件。

综上所述，利用HIF-1α干预BMSCs向成骨-成血管分化，可成功在体外构建三维预血管化的成骨膜片，为骨的再生修复提供新思路。

【Author contributions】 Zhang D performed the experiments, analyzed the data and wrote the article. Huang YL, Teng YH and Han C participated in the study design and reviewed the article. All authors read and approved the final manuscript as submitted.

参考文献

[1] Wang Z, Han L, Zhou Y, et al. The combination of a 3D-Printed porous Ti-6Al-4V alloy scaffold and stem cell sheet technology for the construction of biomimetic engineered bone at an ectopic site [J]. Mater Today Bio, 2022, 16: 100433. doi: 10.1016/j.mtbio.2022.100433.

[2] Thorp H, Kim K, Bou-Ghannam S, et al. Enhancing chondrogenic potential *via* mesenchymal stem cell sheet multilayering[J]. Regen Ther, 2021, 18: 487-496. doi: 10.1016/j.reth.2021.11.004.

[3] Simunovic F, Finkenzeller G. Vascularization strategies in bone tissue engineering[J]. Cells, 2021, 10(7): 1749. doi: 10.3390/cells10071749.

[4] Su ZP, Tian L, Shang HT, et al. Experimental study on the bone morphogenetic protein 1-modified bone marrow mesenchymal stem cell sheets to promote mandibular distraction osteogenesis[J]. Front Surg, 2022, 8: 786351. doi: 10.3389/fsurg.2021.786351.

[5] Wein S, Schemmer C, Al Enezy-Ulbrich MA, et al. Fibrin-based hydrogels with reactive amphiphilic copolymers for mechanical adjustments allow for capillary formation in 2D and 3D environments [J]. Gels, 2024, 10(3): 182. doi: 10.3390/gels10030182.

[6] Li H, Shang Y, Zeng J, et al. Technology for the formation of engineered microvascular network models and their biomedical applications[J]. Nano Converg, 2024, 11(1): 10. doi: 10.1186/s40580-024-00416-7.

[7] Liang J, Zhao J, Chen Y, et al. New insights and advanced strategies for *in vitro* construction of vascularized tissue engineering[J]. Tissue Eng Part B Rev, 2023, 29(6): 692-709. doi: 10.1089/ten.TEB.2023.0044.

[8] Wang Y, Liu M, Zhang W, et al. Mechanical strategies to promote vascularization for tissue engineering and regenerative medicine [J]. Burns Trauma, 2024, 12: tkae039. doi: 10.1093/burnst/tkae039.

[9] Alkazemi H, Mitchell GM, Lokmic-Tomkins Z, et al. Hierarchically vascularized and suturable tissue constructs created through

angiogenesis from tissue-engineered vascular grafts[J]. Acta Biomater, 2024, 189: 168-178. doi: 10.1016/j.actbio.2024.09.052.

[10] 左新慧, 李君, 韩祥祯, 等. 低氧诱导因子-1α对骨髓间充质干细胞成骨分化与血管生成相关因子的影响[J]. 口腔疾病防治, 2021, 29(7): 449-455. doi: 10.12016 /j/issn. 2096-1456.2021.07.003.
Zuo XH, Li J, Han XZ, et al. Effects of hypoxia inducible factor-1α on osteogenic differentiation and angiogenesis related factors of bone marrow mesenchymal stem cells[J]. J Prev Treat Stomatol Dis, 2021, 29(7): 449-455. doi: 10.12016 /j/issn.2096- 1456.2021.07.003.

[11] You J, Liu M, Li M, et al. The role of HIF-1α in bone regeneration: a new direction and challenge in bone tissue engineering[J]. Int J Mol Sci, 2023, 24(9): 8029. doi: 10.3390/ijms24098029.

[12] Chen W, Wu P, Yu F, et al. HIF-1α regulates bone homeostasis and angiogenesis, participating in the occurrence of bone metabolic diseases[J]. Cells, 2022, 11(22): 3552. doi: 10.3390/cells11223552.

[13] 胡小伟, 李琳, 龚荧荧, 等. 补阳还五汤激活PI3K-AKT通路促进氧糖剥夺再灌注损伤的脑微血管内皮细胞血管生成[J]. 浙江大学学报(医学版), 2022, 51(5): 544-551. doi：10.3724/zdxbyxb-2022-0324.
Hu XW, Li L, Gong YY, et al. Buyang Huanwu decoction promotes angiogenesis of rat brain microvascular endothelial cells after oxygen-glucose deprivation reperfusion injury *via* activation of PI3K-AKT signaling pathway[J]. J Zhejiang Univ Med Sci, 2022, 51(5): 544-551. doi: 10.3724/zdxbyxb-2022-0324.

[14] Han Z, He X, Feng Y, et al. Hsp20 promotes endothelial progenitor cell angiogenesis *via* activation of PI3K/Akt signaling pathway under hypoxia[J]. Tissue Eng Regen Med, 2022, 19(6): 1251-1266. doi: 10.1007/s13770-022-00481-1.

[15] Tao JM, Miao R, Liu G, et al. Spatiotemporal correlation between HIF-1α and bone regeneration[J]. FASEB J, 2022, 36(10):e22520. doi:10.1096/fj.202200329RR.

[16] Yasan GT, Gunel-Ozcan A. Hypoxia and hypoxia mimetic agents as potential priming approaches to empower mesenchymal stem cells[J]. Curr Stem Cell Res Ther, 2024, 19(1): 33-54. doi: 10.2174/1574888X18666230113143234.

[18] Chen MH, Wang YH, Sun BJ, et al. HIF-1α activator DMOG inhibits alveolar bone resorption in murine periodontitis by regulating macrophage polarization[J]. Int Immunopharmacol, 2021, 99: 107901. doi: 10.1016/j.intimp.2021.107901.

[19] Shao J, Liu S, Zhang M, et al. A dual role of HIF1α in regulating osteogenesis – angiogenesis coupling[J]. Stem Cell Res Ther, 2022, 13(1): 59. doi: 10.1186/s13287-022-02742-1.

[20] Zhang Y, Huang J, Wang C, et al. Application of HIF-1α by gene therapy enhances angiogenesis and osteogenesis in alveolar bone defect regeneration[J]. J Gene Med, 2016, 18(4/6): 57-64. doi: 10.1002/jgm.2876.

[21] Zhou S, Xiao C, Fan L, et al. Injectable ultrasound-powered bone-adhesive nanocomposite hydrogel for electrically accelerated irregular bone defect healing[J]. J Nanobiotechnology, 2024, 22(1): 54. doi: 10.1186/s12951-024-02320-y.

[22] Wang C, Min S, Tian Y. Injectable and cell-laden hydrogel in the contained bone defect animal model: a systematic review[J]. Tissue Eng Regen Med, 2023, 20(6): 829-837. doi: 10.1007/s13770-023-00569-2.

[23] Zha Y, Li Y, Lin T, et al. Progenitor cell-derived exosomes endowed with VEGF plasmids enhance osteogenic induction and vascular remodeling in large segmental bone defects[J]. Theranostics, 2021, 11(1): 397-409. doi: 10.7150/thno.50741.

[24] Valtanen RS, Yang YP, Gurtner GC, et al. Synthetic and bone tissue engineering graft substitutes: what is the future? [J]. Injury, 2021, 52: S72-S77. doi: 10.1016/j.injury.2020.07.040.

[25] 石剑虹, 田原野, 陈楷, 等. 浓缩生长因子联合骨髓间充质干细胞膜片的生物学性能及其在骨缺损修复中的作用[J]. 吉林大学学报(医学版), 2024, 50(6): 1535-1546. doi: 10.13481/j.1671-587X.20240607.
Shi JH, Tian YY, Chen K, et al. Biological properties of concentrated growth factor combined with bone marrow mesenchymal stem cell sheet and its effect on bone defect repairment[J]. J Jilin Univ Med Ed, 2024, 50(6): 1535-1546. doi: 10.13481/j. 1671-587X.20240607.

[26] Ellermann E, Meyer N, Cameron RE, et al. *In vitro* angiogenesis in response to biomaterial properties for bone tissue engineering: a review of the state of the art[J]. Regen Biomater, 2023, 10: rbad027. doi: 10.1093/rb/rbad027.

[27] Saberi A, Kouhjani M, Mohammadi M, et al. Novel scaffold platforms for simultaneous induction osteogenesis and angiogenesis in bone tissue engineering: a cutting-edge approach[J]. J Nanobiotechnology, 2023, 21(1): 351. doi: 10.1186/s12951-023-02115-7.

[28] Guo R, Morimatsu M, Feng T, et al. Stem cell-derived cell sheet transplantation for heart tissue repair in myocardial infarction[J]. Stem Cell Res Ther, 2020, 11(1): 19. doi: 10.1186/s13287-019-1536-y.

[29] Liu KC, Chen YC, Hsieh CF, et al. Scaffold-free 3D culture systems for stem cell-based tissue regeneration[J]. APL Bioeng, 2024, 8(4): 041501. doi: 10.1063/5.0225807.

[30] Sekine H, Okano T. Capillary networks for bio-artificial three-dimensional tissues fabricated using cell sheet based tissue engineering[J]. Int J Mol Sci, 2020, 22(1): 92. doi: 10.3390/ijms22010092.

[31] Chen J, Zhang D, Li Q, et al. Effect of different cell sheet ECM microenvironment on the formation of vascular network[J]. Tissue Cells, 2016, 48(5):442-451. doi: 10.1016/j. tice. 2016. 08. 002.

[32] Zhang D, Gao P, Li Q, et al. Engineering biomimetic periosteum with β-TCP scaffolds to promote bone formation in calvarial defects of rats[J]. Stem Cell Res Ther, 2017, 8(1):134. doi: 10. 1186/s13287-017-0592-4.

[33] Rui S, Cao ZL, Wang YZ, et al. Characterization of microvessels in the human forehead dermis using intravascular dual perfusion and immunofluorescence staining[J]. Sci Rep, 2025, 15(1): 9717. doi: 10.1038/s41598-025-93752-5.

[34] Zheng P, Huang Z, Tong DC, et al. Frankincense myrrh attenuates hepatocellular carcinoma by regulating tumor blood vessel development through multiple epidermal growth factor receptor-

mediated signaling pathways[J]. World J Gastrointest Oncol, 2022, 14(2): 450-477. doi: 10.4251/wjgo.v14.i2.450.

[35] Docshin P, Bairqdar A, Malashicheva A. Interplay between BMP2 and Notch signaling in endothelial-mesenchymal transition: implications for cardiac fibrosis[J]. Stem Cell Investig, 2023, 10: 18. doi: 10.21037/sci-2023-019.

[36] Merfeld-Clauss S, Lu H, March KL, et al. Notch pathways regulate expression of angiostatic factor activin a in endothelial-pericyte-like mesenchymal stromal cell interactions[J]. Stem Cells Dev, 2023, 32(11/12): 301-313. doi: 10.1089/scd.2023.0003.

[37] Sun J, Shen H, Shao L, et al. HIF-1α overexpression in mesenchymal stem cell-derived exosomes mediates cardioprotection in myocardial infarction by enhanced angiogenesis[J]. Stem Cell Res Ther, 2020, 11(1): 373. doi: 10.1186/s13287-020-01881-7.

[38] Monaci S, Coppola F, Filippi I, et al. Targeting hypoxia signaling pathways in angiogenesis[J]. Front Physiol, 2024, 15: 1408750. doi: 10.3389/fphys.2024.1408750.

[39] Wu D, Liu L, Fu S, et al. Osteostatin improves the Osteogenic differentiation of mesenchymal stem cells and enhances angiogenesis through HIF-1α under hypoxia conditions *in vitro*[J]. Biochem Biophys Res Commun, 2022, 606: 100-107. doi: 10.1016/j.bbrc.2022.02.085.

[40] 付生龙, 张军, 刘俊朋, 等. 骨抑素对大鼠骨髓间充质干细胞增殖、成骨分化和促进血管生成能力的影响[J]. 空军航空医学, 2023, 39(4): 316-321. doi: 10.3969/j. issn. 2097-1753. 2023.04.007.
Fu SL, Zhang J, Liu JP, et al. Effects of ostestatin on proliferation, osteogenic differentiation and angiogenic ability of bone marrow mesenchymal stem cells[J]. Aviat Med Air Force, 2023, 39(4): 316-321. doi: 10.3969/j.issn.2097-1753. 2023.04.007.

[41] Song S, Zhang G, Chen X, et al. HIF-1α increases the osteogenic capacity of ADSCs by coupling angiogenesis and osteogenesis *via* the HIF-1α/VEGF/AKT/mTOR signaling pathway[J]. J Nanobiotechnology, 2023, 21(1): 257. doi: 10.1186/s12951-023-02020-z.

[42] Wang K, Dai X, He J, et al. Endothelial overexpression of metallothionein prevents diabetes-induced impairment in ischemia angiogenesis through preservation of HIF-1α/SDF-1/VEGF signaling in endothelial progenitor cells[J]. Diabetes, 2020, 69(8): 1779-1792. doi: 10.2337/db19-0829.

[43] Zhang Y, Zhang YY, Pan ZW, et al. GDF11 promotes wound healing in diabetic mice *via* stimulating HIF-1α-VEGF/SDF-1α-mediated endothelial progenitor cell mobilization and neovascularization[J]. Acta Pharmacol Sin, 2023, 44(5): 999-1013. doi: 10.1038/s41401-022-01013-2.

[44] Korbecki J, Kojder K, Kapczuk P, et al. The effect of hypoxia on the expression of CXC chemokines and CXC chemokine receptors-a review of literature[J]. Int J Mol Sci, 2021, 22(2): 843. doi: 10.3390/ijms22020843.

[45] 陈佳, 杨艺强, 胡晨, 等. 人骨髓间充质干细胞复合人脐静脉内皮细胞构建预血管化成骨细胞膜片[J]. 中国组织工程研究, 2020, 24(31): 4934-4940. doi: 10.3969/j.issn.2095-4344.2129.
Chen J, Yang YQ, Hu C, et al. Fabrication of prevascularized osteogenic differentiated cell sheet based on human bone marrow mesenchymal stem cells and human umbilical vein endothelial cells[J]. Chin J Tissue Eng Res, 2020, 24(31): 4934-4940. doi: 10.3969/j.issn.2095-4344.2129.

[46] Alcorta-Sevillano N, Macías I, Infante A, et al. Deciphering the relevance of bone ECM signaling[J]. Cells, 2020, 9(12): 2630. doi: 10.3390/cells9122630.

[47] Lee SY, Kim SJ, Park KH, et al. Differential but complementary roles of HIF-1α and HIF-2α in the regulation of bone homeostasis [J]. Commun Biol, 2024, 7(1): 892. doi: 10.1038/s42003-024-06581-z.

[48] Burger MG, Grosso A, Briquez PS, et al. Robust coupling of angiogenesis and osteogenesis by VEGF-decorated matrices for bone regeneration[J]. Acta Biomater, 2022, 149: 111-125. doi: 10.1016/j.actbio.2022.07.014.

[49] Schott NG, Friend NE, Stegemann JP. Coupling osteogenesis and vasculogenesis in engineered orthopedic tissues[J]. Tissue Eng Part B Rev, 2021, 27(3): 199-214. doi: 10.1089/ten.TEB.2020.0132.

（编辑　罗燕鸿，曾曙光）

官网